



ELSEVIER

Journal of Electron Spectroscopy and Related Phenomena 127 (2002) 117–123

JOURNAL OF
ELECTRON SPECTROSCOPY
and Related Phenomena

www.elsevier.com/locate/elspec

Narrow bands and electronic structure in unconventional high- T_C superconductors

E. Cappelluti^{a,c}, C. Grimaldi^b, L. Pietronero^{a,c,*}, S. Strässler^b

^a*Dipartimento di Fisica, Università di Roma I 'La Sapienza', Piazzale A. Moro 2, 00185 Rome, Italy*

^b*Département de Microtechnique–IPM, École Polytechnique Fédérale de Lausanne, CH-1015 Lausanne, Switzerland*

^c*INFM, Unità di Roma 1, Rome, Italy*

Abstract

Electronic structure details play a marginal role in the superconductive properties of conventional superconductors. Electronic energies are by far the most important in these materials and the only relevant electronic parameter, with respect to superconductivity, is essentially the density of states $N(0)$. Cooper oxides and fullerene compounds are characterized by narrow band dispersions and by electronic structures of hundreds meV. This feature is reflected in the high sensitivity of these materials to fine tuning of electron quantities, as shown by the phase diagram of these materials. A similar situation is encountered in recently discovered superconducting MgB_2 , where the Fermi edge lies only ~ 0.5 eV below the top of the σ -bands. We discuss the relevance of these low electronic energy scales in the context of the theory of nonadiabatic electron–phonon coupling, which is achieved when Fermi energies are of the same order as phonon frequencies.

© 2002 Elsevier Science B.V. All rights reserved.

A popular concept in solid state physics is the ‘quasi-particle’ picture, where the important problem of electrons interacting each other and with the lattice dynamics (phonons) is described in terms of non-interacting particles (the quasi-particles) with renormalized effective electronic parameters. This enormous simplification relies on two fundamental approximations. On the one hand, electron–electron interaction is usually disregarded by virtue of the Landau–Fermi liquid picture which assures the imaginary part of the electron–electron self-energy to be much smaller than the real part: $\text{Im}\Sigma_{ei} \sim 1/\tau \ll \text{Re}\Sigma_{ei} \sim E_F$, where τ is the electron lifetime and E_F is the characteristic electron energy scale which can be identified with the Fermi energy. On the other

hand, electron–ion interaction is usually treated by Born–Oppenheimer-like approximations which permit, in adiabatic regime $E_F \gg \omega_{ph}$, to separate electron and lattice degrees of freedom. Here ω_{ph} represents the characteristic energy scale of the phonon spectrum. A common feature of both the theoretical pictures is thus the assumption of a electron energy scale much larger than any other one, $E_F \gg \omega_{ph}$, $1/\tau$, T (T being the temperature). In this situation, only states close to the Fermi level will be probed and the physical properties of the system will not depend on the overall complex electronic structure but just on few parameters related to the Fermi level, as the electron density of states $N(0)$, the Fermi velocity v_F , etc.

The case of electron–phonon interaction can be considered representative. The generic expression of the electron–phonon self-energy reads:

*Corresponding author. Fax: +39-06-446-3158.

E-mail address: luciano.pietronero@roma1.infn.it (L. Pietronero).

$$\Sigma_{\text{ph}}(k) = - \int dq G(k+q) D(q) \Gamma(k+q, q) \quad (1)$$

where G is the one-electron propagator, D the phonon Green's function and Γ the total electron–phonon vertex function. It is often useful to split the total vertex function Γ into a zero order constant term plus higher order vertex corrections, denoted by P , namely:

$$\Gamma(k+q, q) = 1 + P(k+q, q). \quad (2)$$

The many-body nature of the electron–phonon problem is thus hidden in the unknown function Γ which in principle does not have an analytic expression. The feasibility of the standard theory of the electron–phonon, therefore, relies strongly on the adiabatic assumption which can be cast in Green's function formalism in terms of Migdal's theorem. Migdal [1] was indeed able to show in the late 1950s that first order vertex corrections P , shown in Fig. 1, scale to zero with the adiabatic ratio $\omega_{\text{ph}}/E_{\text{F}}$, namely:

$$P(k+q, q) \propto \lambda \frac{\omega_{\text{ph}}}{E_{\text{F}}} \quad (3)$$

where λ is the electron–phonon coupling constant. In the following, for sake of simplicity, the vertex correction P to Migdal's theorem will be denoted without any specification as vertex function, to be not confused with the total vertex Γ which include

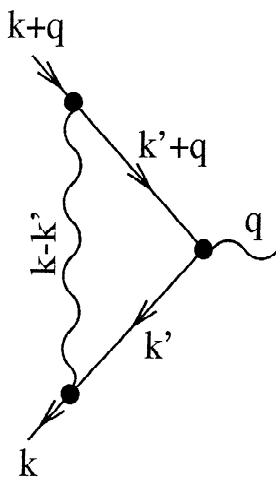


Fig. 1. Diagrammatic representation of the first order electron–phonon vertex correction.

the zero order. In common metals and conventional low temperature superconductors adiabatic ratio is quite small, $\omega_{\text{ph}}/E_{\text{F}} \sim 10^{-3}$, and vertex corrections P are thus negligible.

The huge simplification of Migdal's theorem was on the basis of the following Migdal–Eliashberg (ME) theory of the electron–phonon interaction which was successful to describe many properties of metals and low temperature superconductors [2]. Electron–phonon self-energy at low energy simply reads:

$$\Sigma_{\text{ph}}(\omega) = -\lambda\omega \quad (4)$$

and the coherent part of the Green's function can be written as:

$$G(\mathbf{k}, \omega) = \frac{1}{Z} \frac{1}{\omega - \epsilon(\mathbf{k})/Z} \quad (5)$$

where Z is the electron–phonon renormalization factor connected to the electron–phonon coupling constant $\lambda = 2g^2N(0)/\omega_{\text{ph}}$ by $Z = 1 + \lambda$. It is easy to see from Eq. (5) that ME theory leads thus to an effective renormalization by the factor $1 + \lambda$ of many physical properties of the system, as the Fermi velocity $v_{\text{F}}^* = v_{\text{F}}/(1 + \lambda)$, the electron mass $m^* = m(1 + \lambda)$ or the electron specific heat $\gamma = (1 + \lambda) 2\pi^2N(0)/3$ [3].

An interesting point worth to be stressed here is that in this standard ME approach based on the adiabatic theory electron–phonon interaction depends on the electronic structure only through the density of states at the Fermi level $N(0)$ which appears in the definition of λ . The low sensitivity of ME theory to electron structure details actually allowed for an easy experimental check of the theoretical predictions in real compounds. For instance, the superconducting critical temperatures T_{C} of many conventional materials could be quantitative predicted by using the McMillan formula:

$$T_{\text{C}} = \frac{\omega_{\text{ph}}}{1.2} \exp \left[- \frac{1.04(1 + \lambda)}{\lambda - \mu^*(1 + 0.62\lambda)} \right] \quad (6)$$

where μ^* measures the screened Coulomb repulsion, and good agreement was found with the experimental values. In this context, a theoretical upper limit of $T_{\text{C}} \leq 20 - 25$ K was however expected, and research activity on superconductivity in the 1970s was

mainly addressed to optimize the ME theory and to approach this limit [4].

The conventional picture of metals and superconductivity has however been shaken by the discovery of the so-called high- T_C superconductors, which present an anomalous phenomenology in both the superconducting and the normal states. Most evident is of course the high critical temperature which ranges up to $T_C=130$ K in cuprates and up to $T_C=40$ K in alkali doped fullerenes, well beyond the ME limit of $T_C=20$ – 25 K. The recent discovery of superconductivity with $T_C\approx 39$ K in MgB_2 suggests that also this material should be included in the high- T_C family [5].

High- T_C compounds can be regarded however as unconventional also with respect to other points of view. For instance charge carrier density and Fermi energy E_F are both small in these materials [6]. These features, all together with the high values of the critical temperature, appear difficult to reconcile within the ME framework. In a textbook example of a common broad band metal indeed low density of carriers and small E_F can be achieved in almost empty (filled) electron (hole) bands. This does not seem however the case of these systems. In addition, it should be reminded that this situation is accompanied by a vanishing density of states and the corresponding superconductive pairing is expected to be suppressed (Fig. 2a).

On the contrary high- T_C materials are characterized by very narrow band electronic structures. In this situation small Fermi energies can be naturally accounted for regardless the filling level (Fig. 2b). However density of states $N(0)$ in these systems is not particularly high and it is hard to think about such compounds as the best optimized ME superconductors. This observation suggest that new physics is induced in narrow band systems.

An interesting insight comes from the comparison of the electronic energy scales with the lattice (phononic) ones. Estimates of the Fermi energy in cuprates and fullerenes give, respectively, $E_F\sim 0.35$ eV and $E_F\sim 0.25$ eV, to be compared with the highest phonon modes $\omega_{\text{ph}}\sim 90$ meV in cuprates and $\omega_{\text{ph}}\sim 200$ in fullerenes. In this context the adiabatic parameter appears to be not at all negligible, $\omega_{\text{ph}}/E_F\sim 0.3$ – 0.8 , and one of the assumptions of Migdal–Eliashberg theory, the adiabatic hypothesis, breaks

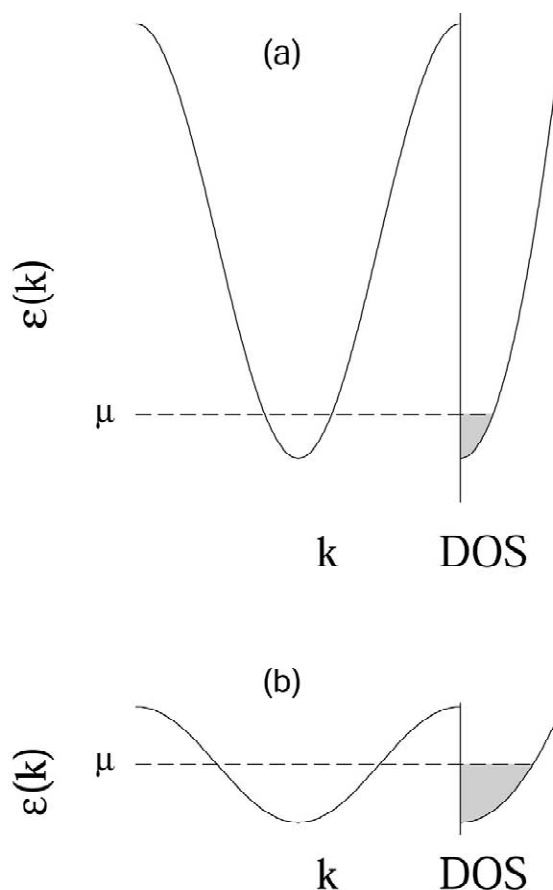


Fig. 2. Schematic electronic structure of: (a) an almost empty broad band; (b) a half-filled narrow band. Both the systems are characterized by small Fermi energies.

down. The use of the conventional theory is thus intrinsically inconsistent and the explicit inclusion of nonadiabatic effects needs to be taken into account. We are going to see that the onset of nonadiabatic effects opens new channels of electron–phonon interaction that drastically affect the normal and superconducting state phenomenology of these materials.

From a technical point of view the definition of a electron–phonon theory valid in nonadiabatic regime where Migdal’s theorem does not apply is a highly difficult task. In the extreme limit of antiadiabatic regime, $E_F\ll\omega_{\text{ph}}$, polaron formation is expected which will eventually undergo self-trapping localization. This kind of description would be therefore best suited for insulating phases. On the other hand,

metallic properties are well established in the normal state of high- T_C compounds.

A most appropriate starting point in our opinion is thus a perturbative scheme where nonadiabatic vertex corrections arising from the breakdown of Migdal's theorem are taken into account up to the first order. This approach, valid as far as the magnitude of the vertex corrections is small $\lambda\omega_{\text{ph}}/E_F < 1$, is thought to properly describe systems in weakly nonadiabatic regime where conventional metallic properties are indeed significantly modified by nonadiabatic effects but not yet destroyed. A controlled theory can be built up by counting the number of nonadiabatic vertex corrections both in normal and superconducting states [7]. The diagrammatic representation of the superconducting equations in nonadiabatic regime is shown in Fig. 3, where only first order nonadiabatic corrections appear. The electron–phonon normal state self-energy is shown in panel (a), while in panel (b) the electron–electron interaction leading to the Cooper pairing is depicted. Only the first diagram on the right side of each panel would survive in adiabatic regime. The inclusion of nonadiabatic diagrams gives rise new channels of electron–phonon interaction, represented by the ad-

ditional diagrams not included in the adiabatic scheme. Electronic properties as well as superconductive ones are thus expected to be strongly modified. In particular, it is of major interest to assess to which extent nonadiabatic channels can favour or disfavour the superconducting pairing. In order to clarify this point a microscopic analysis of the vertex function, which represents the nonadiabatic key element of the superconducting equations, is needed.

The vertex function, diagrammatically shown in Fig. 1, can be analytically evaluated by using Green's function formalism. Its explicit expression reads [1,8]:

$$P(\omega_n, \omega_m; \mathbf{q}) = g^2 \sum_{\mathbf{p}, \omega_l} D(\omega_n - \omega_l) G(\mathbf{p}, \omega_l) G(\mathbf{p} + \mathbf{q}, \omega_l + \omega_m) \quad (7)$$

where ω_n and ω_m are, respectively, the incoming and outgoing electronic frequency in Matsubara space and \mathbf{q} is the exchanged phonon momentum. The vertex function $P(\omega_n, \omega_m; \mathbf{q})$ was shown to be quite insensitive to the electronic frequencies ω_n and ω_m considered separately, while it shows a strong dependence on the the exchanged momentum \mathbf{q} and frequency $\omega_q = \omega_n - \omega_m$, where \mathbf{q} and ω_q are generic momenta and frequencies characteristic of the phonon spectrum [7,8]. The complex momentum–frequency structure can be schematized by the representative static (P_s) and dynamic (P_d) limits, defined as $P_s = \lim_{\mathbf{q} \rightarrow 0, \omega_q \rightarrow 0} P$ and $P_d = \lim_{\omega_q \rightarrow 0, \mathbf{q} \rightarrow 0} P$. It can be shown in full generality that static and dynamic limits are, respectively, negative and positive, namely $P_s < 0$, $P_d > 0$. Their actual values however will depend on specific properties of the system (density of states, electron/phonon energies, etc.).

Determination of the total sign of the vertex corrections is a very important issue since a positive sign induces an effective enhancement of the superconducting pairing and a negative one a suppression [9]. The sign of the vertex function for a representative simple case (Einstein phonon with energy ω_0 , half-filled constant DOS band) is plotted in Fig. 4. As shown in that picture the vertex function sign is not univocally determined in the whole $\mathbf{q} - \omega_q$ space but is depends on the particular range of momenta and frequencies actually probed by the electron–

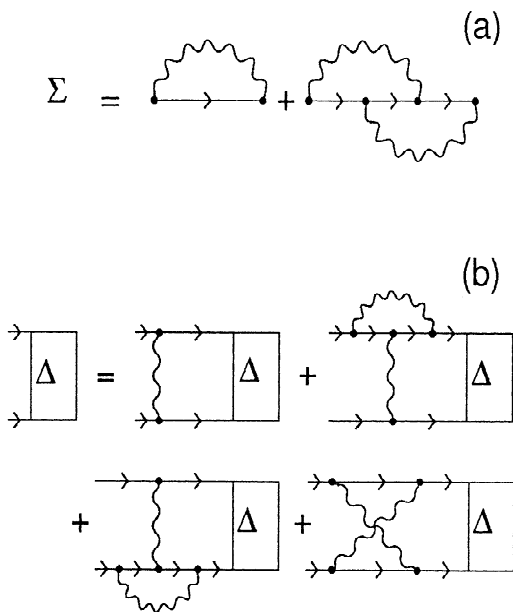


Fig. 3. Nonadiabatic electron–phonon coupling: (a) normal state self-energy; (b) Cooper pairing.

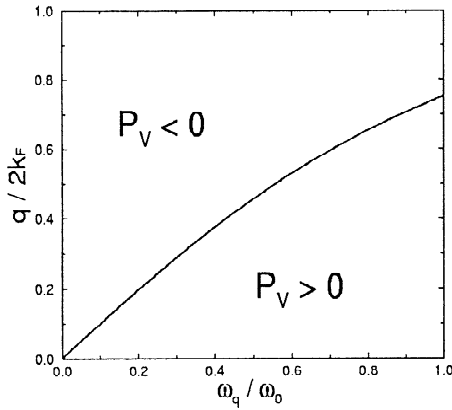


Fig. 4. Sign of the vertex function in the space of exchanged momenta and frequencies.

phonon interaction. In particular we can expect that a predominance of small \mathbf{q} scattering will favour positive parts of the vertex function and will lead to a net increase of the critical temperature with respect to the adiabatic ME predictions [9].

Strong evidences suggest that this could be the case of high- T_C materials [10]. Narrow bands and small Fermi energies indeed, while on one hand give rise nonadiabatic effects, on the other hand imply strong electronic correlation as soon as the electronic kinetic energy, parametrized by E_F becomes comparable with the on-site Coulomb repulsion U . As a consequence, electron scattering with charge fluctuations, as phonons, is strongly suppressed. To understand this point one should keep in mind that in this situation electrons cannot be considered as independent quantities but they will result to be dressed by the so-called ‘correlation hole’ which suppresses electron density within a sphere of radius ξ , where ξ is the correlation length (Fig. 5). Charge modulations with wavelength smaller than ξ , or equivalent momentum larger than ξ^{-1} , are thus not coupled providing an upper cut-off in the momenta space $q_c \sim \xi^{-1}$ which measures the degree of the electronic correlation: the stronger the correlation effects the smaller q_c . In this situation electron phonon nonadiabatic channels mainly probe the small \mathbf{q} positive region of the vertex function a strengthening of the superconducting Cooper pairing is expected. As a result, high critical temperature values can be achieved with reasonable electron–phonon coupling

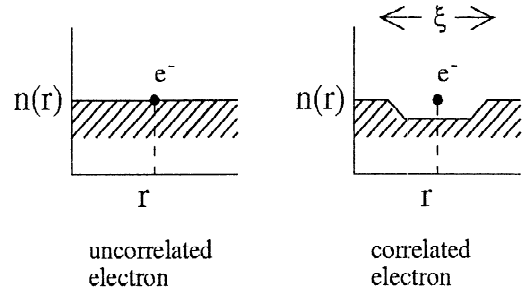


Fig. 5. Schematic diagram of uncorrelated and correlated electrons.

$\lambda < 1$ well beyond the theoretical upper ME limit $T_C \leq 20\text{--}25$ K without assuming unphysically large $\lambda \gg 1$.

To quantify this concept, we have numerically solved the modified superconducting equations in nonadiabatic regime represented in Fig. 3. Their analytical expression reads [7,9]:

$$Z(\omega_n) = 1 + \frac{T_C}{\omega_n} \sum_{\omega_m} \Gamma_Z(\omega_n, \omega_m, Q_c) \eta_m \quad (8)$$

$$Z(\omega_n) \Delta(\omega_n) = T_C \sum_{\omega_m} \Gamma_\Delta(\omega_n, \omega_m, Q_c) \frac{\Delta(\omega_m)}{\omega_m} \eta_m \quad (9)$$

where $\eta_m = 2 \arctan\{E_F/[Z(\omega_m)\omega_m]\}$, $Z(\omega_n)$ is the renormalization function and $\Delta(\omega_n)$ is the superconducting gap function in Matsubara frequencies. The breakdown of Migdal’s theorem strongly affects the ‘on-diagonal’ Γ_Z and the ‘off-diagonal’ Γ_Δ electron–phonon kernels which include now vertex and the ‘so-called’ cross corrections [7]:

$$\begin{aligned} \Gamma_Z(\omega_n, \omega_m, Q_c) &= \lambda D(\omega_n - \omega_m) [1 + \lambda P(\omega_n, \omega_m, Q_c)] \\ \Gamma_\Delta(\omega_n, \omega_m, Q_c) &= \lambda D(\omega_n - \omega_m) [1 + 2\lambda P(\omega_n, \omega_m, Q_c)] \\ &\quad + \lambda^2 C(\omega_n, \omega_m, Q_c) - \mu \end{aligned}$$

where $D(\omega_n - \omega_m)$ is the phonon propagator, μ the unscreened Coulomb repulsion (to be not confused with the chemical potential) which is related to the screened Coulomb pseudopotential μ^* through the relation $\mu^* = \mu/[1 + \mu \ln(E_F/\omega_{ph})]$. $P(\omega_n, \omega_m, Q_c)$ and $C(\omega_n, \omega_m, Q_c)$ represent at proper average of the nonadiabatic vertex and cross functions over the momentum space probed by the electron–phonon scattering, parametrized by the quantity Q_c [7,9].

The example of fullerene compounds can be

indicative of the enhancement of T_C with respect to the critical values predicted for the same microscopic parameters λ , ω_{ph} , μ [11]. Indeed, best accuracy measurements of the carbon isotope coefficient α in Rb_3C_{60} give $\alpha=0.21$ [12]. The small value of α suggests a strong Coulomb repulsion which should compete with λ . In such a situation strong values of λ would be necessary to account for $T_C=30$ K in Rb_3C_{60} . In Fig. 6 we show the numerical solutions of both the adiabatic Migdal–Eliashberg and the nonadiabatic theory constrained to reproduce the experimental values $T_C=30$ K and $\alpha=0.21$ with an Einstein phonon ω_{ph} . For given values of ω_{ph} lying in the physical range of the fullerene phonon spectrum $\omega_{\text{ph}} < 2300$ K, a extremely large electron–phonon coupling $\lambda \sim 1 \div 4$ is required in ME theory (filled squares), in contrast with local density approximation results which find $\lambda < 1$. On the other hand, the same experimental data are fitted in the nonadiabatic theory (open triangles) with much more reasonable values of λ in good agreement with the theoretical calculations [11].

To summarize, in our opinion the origin of the high- T_C mechanism in these unconventional materials characterized by narrow bands relies more in a

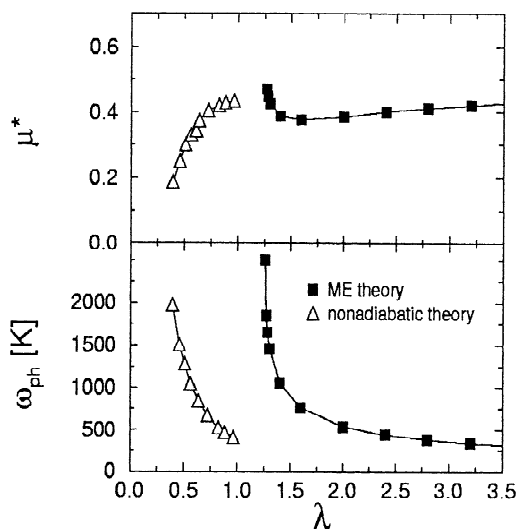


Fig. 6. Phonon frequency ω_{ph} (lower panel) and Coulomb pseudopotential μ^* (upper panel) as functions of the electron–phonon coupling λ . Both the ME (filled squares) and the nonadiabatic (open triangles) equations have been solved in order to reproduce $T_C=30$ K and $\alpha=0.21$.

qualitative different theory based on nonadiabatic interferences than in a quantitative strong value of the electron–phonon superconducting pairing. Along this perspective, looking for additional evidences of a nonadiabatic interaction in other superconducting and normal state properties appear of the highest interest. Characteristic nonadiabatic fingerprints should be sought among those physical features which are qualitatively modified with respect to the conventional ME framework.

Isotope effect measurements are particularly suitable to this aim since they directly probe the retarded nature of the electron–phonon interaction. Nonadiabatic theory, in particular, predicts finite isotope effects on quantities which are not expected to show it. One of them is the electronic effective mass that in ME framework is renormalized by electron–phonon interaction as $m^*(\lambda) = m(1 + \lambda)$. No isotope effect is also expected. Small Fermi energies however introduce an additional dependence on the nonadiabatic parameter ω_{ph}/E_F , $m^* = m^*(\lambda, \omega_{\text{ph}}/E_F)$, which gives rise a finite negative isotope effect on m^* [13]. Finite negative isotope effects on m^* has actually been detected in the underdoped phase of cuprates [14]. We think that the experimental observation of such an isotope effect is a direct evidence of the nonadiabatic nature of the electron–phonon coupling in unconventional superconductors.

Another measurable quantity which could unveil signatures of nonadiabaticity is the normal state Pauli susceptibility χ . In the adiabatic regime χ is expected to be completely unaffected by the electron–phonon interaction. Conversely, when nonadiabatic channels are operative, χ acquires a dependence on λ and on ω_{ph} which could be detected by suitable experiments, in particular by isotope substitution effects [15]. The observation of an isotope effect on χ , absent in ME regime, represents a stringent test of the nonadiabatic hypothesis.

A further interesting nonadiabatic feature appearing in small E_F materials is the response of the superconducting state to disorder and non-magnetic impurities. Within the adiabatic regime, isotropic s -wave superconductors are robust against the presence of weak disorder. In particular, T_C is nearly independent of the amount of disorder [16]. This situation changes when nonadiabatic effects are taken into account. In fact vertex corrections are

quite sensitive to the amount of disorder, and the effective nonadiabatic pairing is reduced. Contrary to the predictions of ME theory, a sizable reduction of T_C upon disorder is expected for a nonadiabatic s -wave superconductor [17]. It is remarkable that a T_C -reduction under radiation induced disorder has actually been reported in fullerenes [18], wave cuprates [19] and in MgB_2 [20].

The reduction of T_C in MgB_2 suggests a nonadiabatic pairing also in this recently discovered superconductor. At first glance, this would be surprising since MgB_2 is expected to be a broad band material. In fact, it is isostructural and iso-electronic with graphite compounds where boron atoms in MgB_2 replacing carbons in graphite. The electronic structure is thus related to the strong boron–boron bond with typical energies of eV units. Fermi energies are expected to be correspondingly much higher than phonon frequencies and ME theory should be well grounded in these materials. However, in our opinion more care is needed.

For instance we can compare the maximum T_C in graphite intercalated compounds (GIC), which was reported to be $T_C=0.55$ K at ambient pressure in agreement with ME predictions [21], with $T_C=39$ K of MgB_2 . The large difference in T_C values between GIC and MgB_2 and the reduction of T_C in MgB_2 upon disorder, therefore, point towards a nonadiabatic pairing even in this broad band compound. To understand in which way this is possible, the specific electronic structure of MgB_2 needs to be taken into account. Two kind of bands cutting the Fermi edge can be identified: two (bonding and antibonding) π -bands with large Fermi energies E_F^π and two almost two-dimensional σ -bands arising from the in-plane $p_{x,y}$ orbitals. In GIC, σ -bands are 2 eV below the Fermi level and do not play any role. However, because of the differently charged boron and magnesium planes, σ -bands in MgB_2 are significantly shifted upwards and cut the Fermi level around the Γ point [22]. The Fermi velocity of these σ -bands is thus quite small, $E_F^\sigma \sim 0.5$ eV, and nonadiabatic effects start to be important. In some regards this situation is similar to panel (a) of Fig. 2, where also nonadiabatic effects were expected to arise. The fundamental difference which makes

MgB_2 somewhat peculiar is however the two-dimensionality of the nonadiabatic bands. In this case in fact density of states remains finite even for the extreme nonadiabatic limit of a Fermi level approaching the top (bottom) of the band, and we expect finite electron–phonon interaction $\lambda \propto N(0)$ even in nonadiabatic regime.

References

- [1] A.B. Migdal, Zh. Éksp. Teor. Fiz. 34 (1958) 1438; A.B. Migdal, Sov. Phys. JETP 7 (1958) 996.
- [2] D.J. Scalapino, in: R.D. Parks (Ed.), The Electron–Phonon Interaction and Strong-Coupling Superconductors, Marcel Dekker, New York, 1969.
- [3] G. Grimvall, The Electron–Phonon Interaction in Metals, North-Holland, Amsterdam, 1981.
- [4] P.B. Allen, B. Mitrovic, Theory of Superconducting T_C , Solid State Physics, Vol. 37, Academic Press, New York, 1982.
- [5] J. Nagamatsu, N. Nakagawa, T. Muranaka, Y. Zenitani, J. Akimitsu, Nature 410 (2001) 63.
- [6] Y.J. Uemura et al., Nature 352 (1991) 605.
- [7] C. Grimaldi, L. Pietronero, S. Strässler, Phys. Rev. B 52 (1995) 10530.
- [8] L. Pietronero, S. Strässler, C. Grimaldi, Phys. Rev. B 52 (1995) 10516.
- [9] C. Grimaldi, L. Pietronero, S. Strässler, Phys. Rev. Lett. 75 (1995) 1158.
- [10] M. Kulić, Phys. Rep. 338 (2000) 1.
- [11] E. Cappelluti, C. Grimaldi, L. Pietronero, S. Strässler, Phys. Rev. Lett. 85 (2000) 4771.
- [12] M.S. Fuhrer, K. Cherrey, A. Zettl, M.L. Cohen, V.H. Crespi, Phys. Rev. Lett. 83 (1999) 404.
- [13] C. Grimaldi, E. Cappelluti, L. Pietronero, Europhys. Lett. 42 (1998) 667.
- [14] G.M. Zhao, K. Conder, H. Keller, K.A. Müller, Nature 381 (1996) 676.
- [15] E. Cappelluti, C. Grimaldi, L. Pietronero, Phys. Rev. B 64 (2001) 025136.
- [16] P.W. Anderson, J. Phys. Chem. Solids 11 (1959) 26.
- [17] M. Scattoni, C. Grimaldi, L. Pietronero, Europhys. Lett. 47 (1999) 588.
- [18] S.K. Watson et al., Phys. Rev. B 55 (1997) 3866.
- [19] S.I. Woods et al., Phys. Rev. B 58 (1998) 8800.
- [20] A.E. Karkin et al., JETP Letters 73 (2001) 570.
- [21] M.S. Dresselhaus, G. Dresselhaus, Adv. Phys 30 (1981) 139, For a comprehensive review about graphite and graphite intercalated compounds.
- [22] J.M. An, W.E. Pickett, Phys. Rev. Lett. 86 (2001) 4366.